nature cell biology

SUPPLEMENTARY INFORMATION

https://doi.org/10.1038/s41556-019-0337-y

In the format provided by the authors and unedited.

RPEL-family rhoGAPs link Rac/Cdc42 GTP loading to G-actin availability

Jessica Diring[1], Stephane Mouilleron[2], Neil Q. McDonald[3,4] and Richard Treisman[1]*

[1]Signalling and Transcription Group, The Francis Crick Institute, London, UK. [2]Structural Biology Science Technology Platform, The Francis Crick Institute, London, UK. [3]Signalling and Structural Biology Group, The Francis Crick Institute, London, UK. [4]Institute of Structural and Molecular Biology, Department of Biological Sciences, Birkbeck College, London, UK. *e-mail: richard.treisman@crick.ac.uk

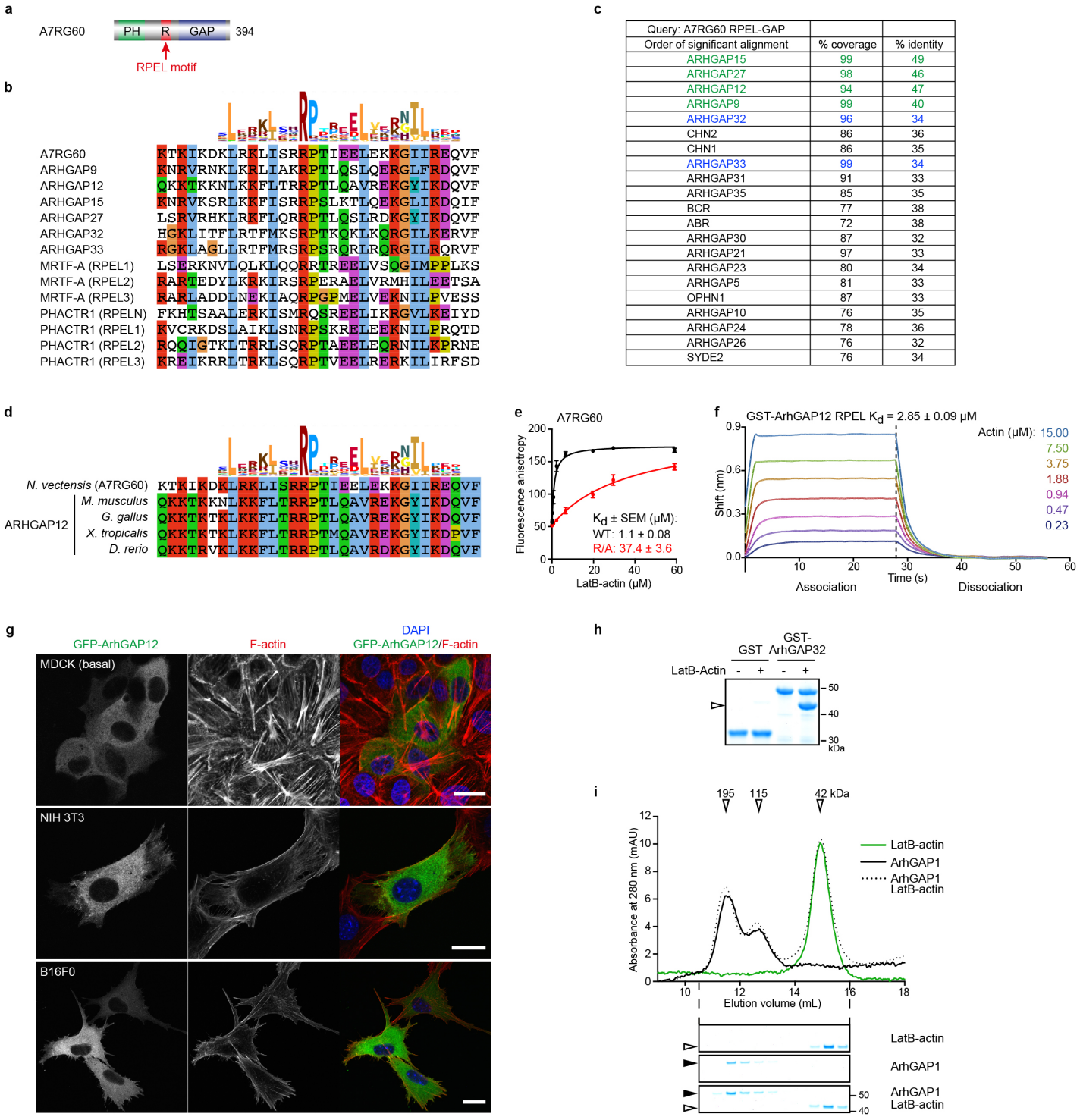

Supplementary Figure 1

The ArhGAP12 and ArhGAP32 families of rhoGAPs are RPEL proteins.

(**a**) Domain structure of the *Nematostella vectensis* A7RG60 GAP protein. (**b**) Clustal X sequence alignment of the canonical RPEL motif from *Nematostella vectensis* A7RG60, the atypical RPEL motifs of ArhGAP12/32 family GAPs, and representative MRTF and PHACTR family RPEL motifs, aligned with the Pfam PF02755 HMM logo. (**c**) Protein blast of mouse RefSeq database using A7RG60 RPEL-GAP sequence. (**d**) Clustal X sequence alignment of the canonical RPEL motif from *Nematostella vectensis* A7RG60, with the atypical RPEL motifs conserved in ArhGAP12 homologs across vertebrate evolution. (**e**) Fluorescence anisotropy analysis of LatB-actin binding to the FAM-conjugated A7RG60 RPEL peptide in (b) or a derivative in which the core RPEL arginine is replaced by alanine. Dissociation constants (K_d) were derived from the non-linear regression fit of the data points. Data represent means ± SEM, *n*=6 independent experiments. (**f**) Octet biolayer interferometry assay. Biosensors loaded with GST-RPEL^{ArhGAP12} were incubated with different concentrations of G-actin, which was washed out at 28s (dotted line). K_d is mean ± SEM, *n*=6 independent experiments; a representative experiment is shown. **(g)** Confocal imaging of transiently expressed GFP-ArhGAP12 and endogenous F-actin in growing MDCK cells (basal section) and serum-stimulated (15% FCS, 10 min) NIH 3T3 or B16F0 cells. F-actin and DNA were counterstained with Phalloidin and DAPI respectively. Representative images of three independent experiments. Scale bar, 20 µm. (**h**) Immobilised recombinant GST and GST-ArhGAP32 RPEL-GAP proteins were used to recover purified LatB-actin from solution; actin recovery was analysed by SDS-PAGE/Coomassie blue staining. Representative data of three experiments. (**i**) Analytical gel filtration. Elution profiles of recombinant GST-ArhGAP1 (4 µM) and purified LatB-actin (2 µM) either alone (solid lines) or in a mixture (dotted line), analysed by absorbance (top) or SDS-PAGE/Coomassie blue staining (bottom). Apparent M_r are indicated. Black and open horizontal arrowheads point to ArhGAP1 and actin respectively. Data are from one of three independent experiments. Source data for e, f and i are shown in Supplementary Table 1. Unprocessed Coomassie gels are shown in Supplementary Figure 8.

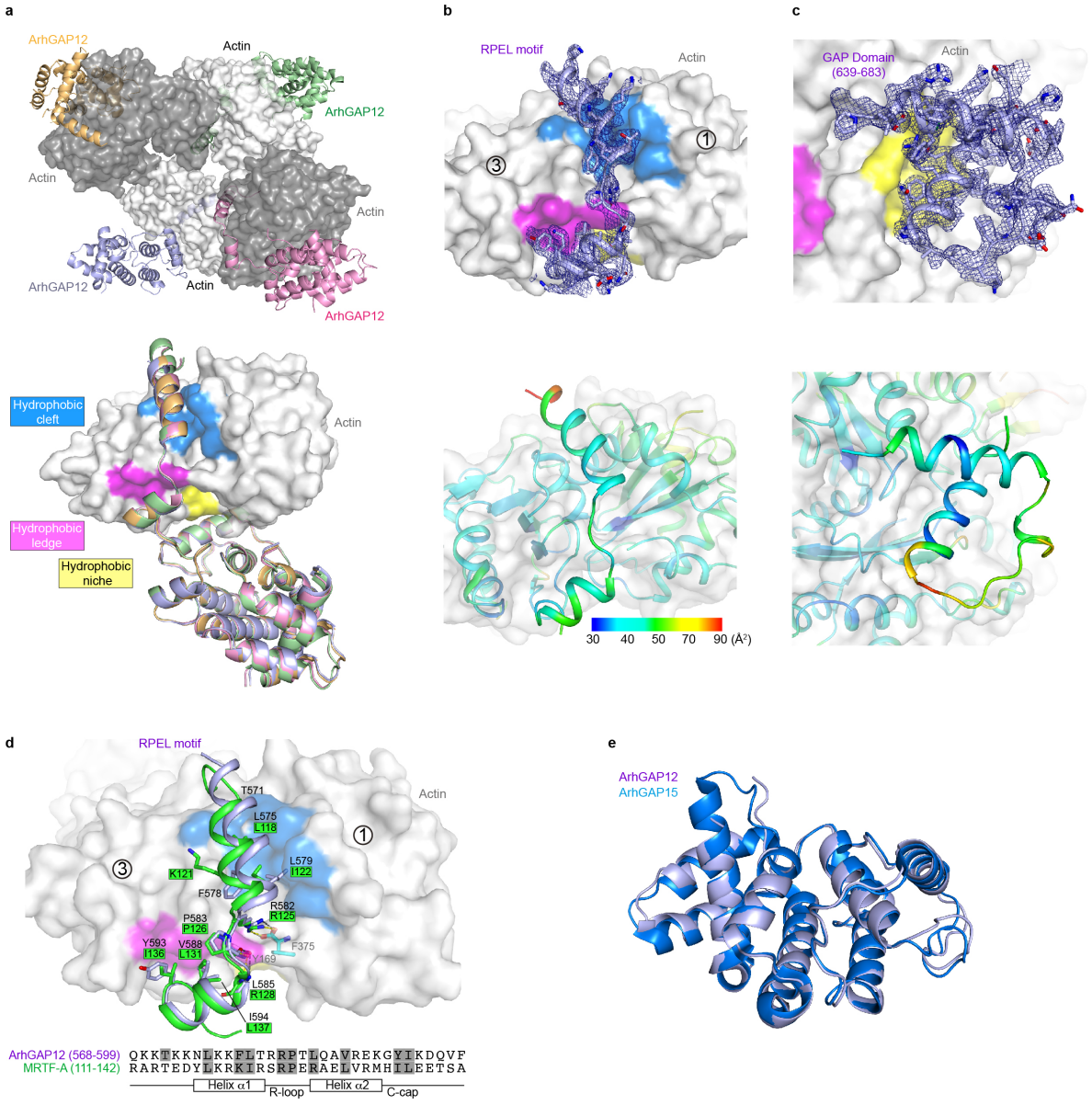

Supplementary Figure 2

Structural analysis of the ArhGAP12/G-actin complex.

(**a**) Top, the asymmetric unit comprises four copies of the ArhGAP12/G-actin complex; bottom, overlay of the four ArhGAP12/G-actin units. (**b**) RPEL-actin binding contacts: top, 2Fobs-Fcalc electronic density map, contoured at 1σ, level of the ArhGAP12 RPEL motif bound to the actin hydrophobic cleft (blue) and ledge (pink); bottom, same view with the secondary structure color coded according to the B-factor values from blue (low) to red (high). (**c**) GAP domain (residues 639-683)-actin binding contacts: Top, 2Fobs-Fcalc electronic density map; bottom, B-factor values. Data presented as in (b). (**d**) Superposition of ArhGAP12^{RPEL} (blue) and MRTF-A^{RPEL2} (green, PDB 2V52, ref[13]) in complex with G-actin (grey) reveals that all the typical contacts with actin are conserved in the RPEL-like motif of ArhGAP12. Schematic highlights residues that make contacts with actin (grey) and shows secondary structure elements. (**e**) Superposition of the ArhGAP12 and ArhGAP15 (PDB 3BYI) structures. (**f**) Octet biolayer interferometry assay. Biosensors loaded with the indicated GST-ArhGAP12 ΔNΔP derivatives were incubated with different concentrations of G-actin, which was washed out at the indicated times (dotted lines). K_d are means ± SEM, *n*=5 (R582A), *n*=8 (Q646A F650A H654A) independent experiments; representative experiments are shown. GST-ArhGAP12 ΔNΔP R582A Q646A F650A H654A could not be quantified under these assay conditions. Source data for f are shown in Supplementary Table 1.

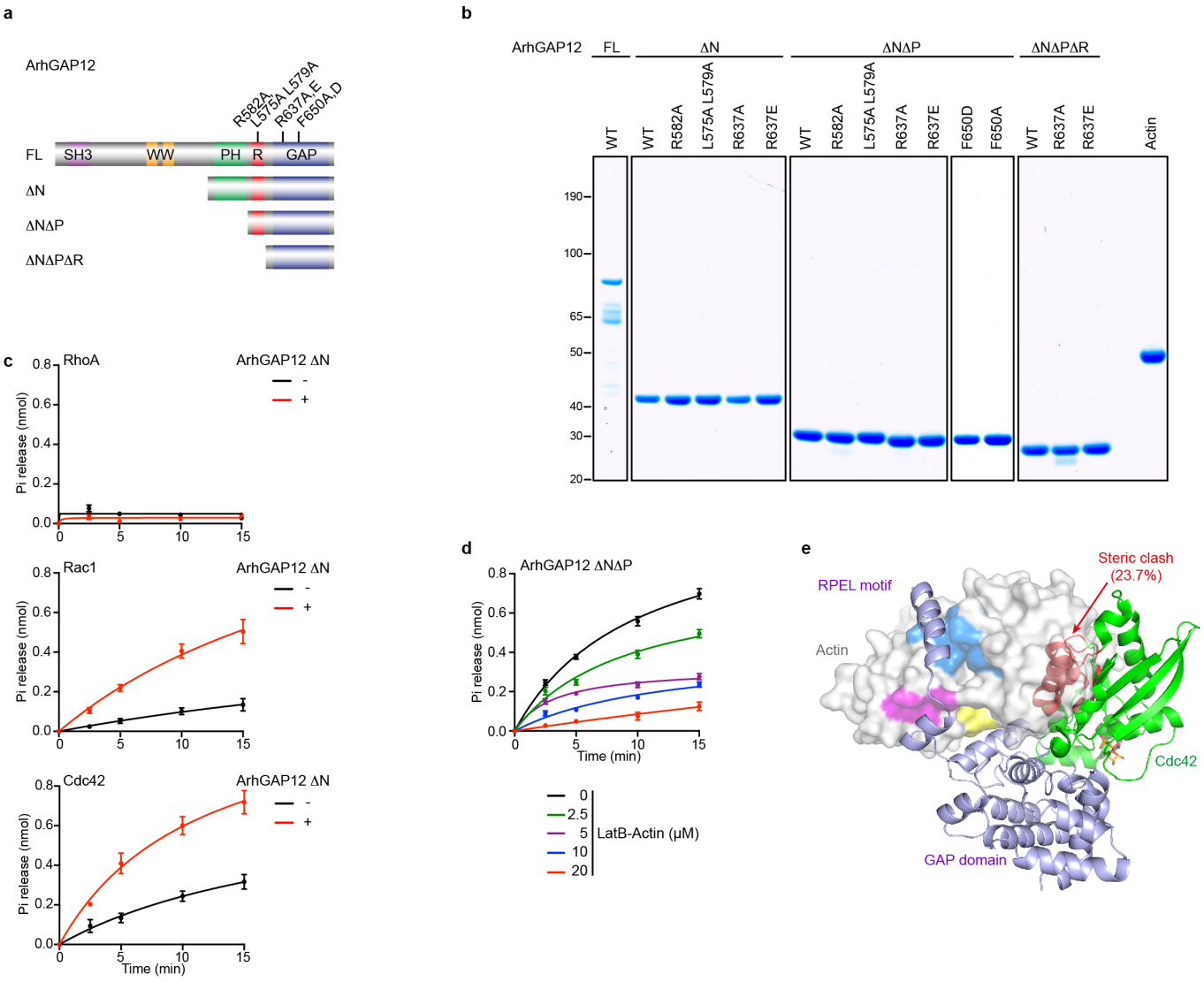

Supplementary Figure 3

Actin inhibits ArhGAP12 GAP activity towards Rac and Cdc42.

(**a**) ArhGAP12 derivatives: full-length (FL, amino acids 1-791); N-terminal truncations ΔN (410-791), ΔNΔP (568-791), and ΔNΔPΔR (582-791); and point mutant derivatives (R582A, L575A L579A, R637A/E, F650A/D). (**b**) Purified recombinant ArhGAP12 derivatives (1.2 μg) with rabbit actin, analysed by SDS-PAGE and Coomassie blue staining. (**c**) GAP assay, measuring Pi release, with Rac1, Cdc42 and RhoA. (**d**) Inhibition of ArhGAP12 Rac GAP activity by increasing concentrations of LatB-actin. (**c,d**) Data (means ± SEM, *n*=4 independent experiments) were fitted by non-linear regression. (**e**) Model of Cdc42 bound to ArhGAP12. The GAP domain of the MgcRacGAP/Cdc42.GDP structure (PDB ID 5C2J) was superimposed onto the GAP domain of the ArhGAP12 ΔNΔP/actin structure. Exposed and occluded Cdc42 residues are shown as green and red ribbons, GDP in orange. Occlusion of Rac1 is displayed in Figure 4d. Source data for c and d are shown in Supplementary Table 1.

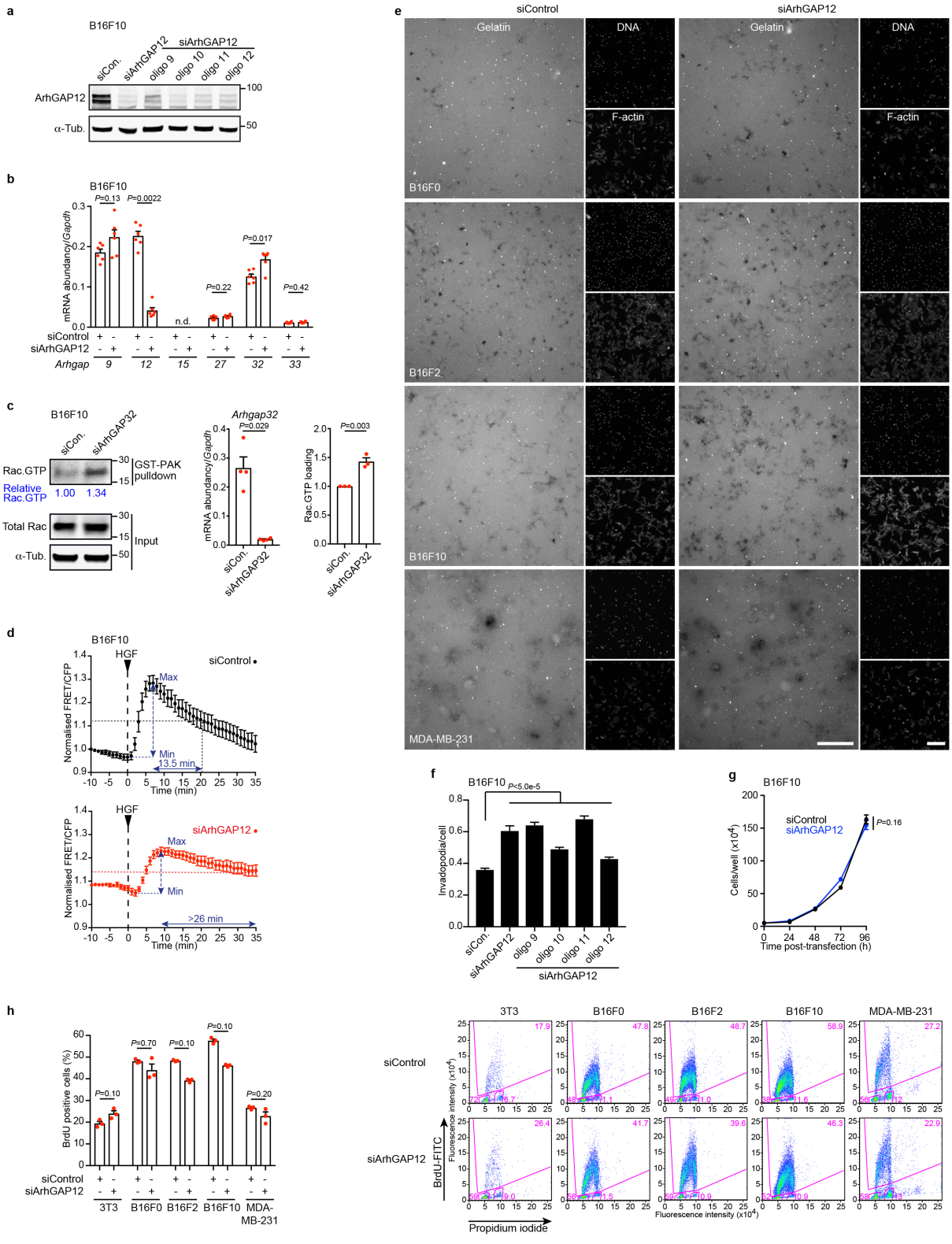

Supplementary Figure 4

ArhGAP12 controls Rac activity and Rac-dependent processes in B16 melanoma and MDA-MB-231 carcinoma cells.

Cells were transfected with control or ArhGAP12 siRNA. (**a**) Representative immunoblot of three independent experiments showing the level of ArhGAP12 knockdown upon deconvolution of the pool of four RNAi oligonucleotides in B16F10 cells. (**b**) Expression of the ArhGAP12- and 32-family mRNAs in ArhGAP12-depleted B16F10. The expression of ArhGAP15 was too low to be detected (n.d., not determined). Data are means ± SEM, *n*=6 independent experiments, two-tailed Mann-Whitney test. (**c**) Rac.GTP level was assessed by GST-PAK pulldown in ArhGAP32-depleted B16F10 cells. Left, representative immunoblot. Centre, level of ArhGAP32 knockdown. Data are mean ± SEM, *n*=4 independent experiments, two-tailed Mann-Whitney test. Right, quantification of Rac.GTP loading. Data are mean ± SEM, *n*=3 independent experiments, two-tailed unpaired t test. (**d**) Kinetics of Rac.GTP loading following HGF stimulation of serum-starved B16F10 cells, analysed using the RaichuEV-Rac FRET biosensor for the individual conditions displayed as in Figure 5d. The time to downregulate to 50% of the peak activity for each curve was calculated as t_{50} = t(Min + 50% (Max - Min)) - t(Max) where t represents time, Min the minimum value, Max the maximum value. (**e**) Representative images from three independent experiments of invadopodia formation in B16F0, F2, F10 and MDA-MB-231 cells plated overnight on Oregon-green labelled gelatin, as quantified in Figure 6a. F-actin and DNA were counterstained with Phalloidin and DAPI respectively. Scale bar, 400 µm. (**f**) Invadopodia formation upon deconvolution of the pool of four ArhGAP12 RNAi oligonucleotides in B16F10. 4 fields per well have been imaged and averaged. Data shown represent *n*=24 independent wells pooled from three independent experiments. At least 26,942 cells were imaged per condition. Data are means ± SEM, two-tailed Mann-Whitney test. The first two bars are identical to data displayed in Figure 6b. (**g**,**h**) ArhGAP12 depletion does not affect proliferation. (**g**) Growth curves in B16F10 cells following siRNA transfection. Data are means ± SEM, *n*=3 independent experiments, two-tailed Wilcoxon matched-pairs test. (**h**) Cells were labelled for 2.5h with BrdU and analysed by flow cytometry. Left, graph shows a quantification of BrdU positive cells. Data are means ± SEM, *n*=3 independent experiments, two-tailed Mann-Whitney test. Right, representative plots showing gates and percentages of cells in G1, G2 and S phase. Source data for b-d and f-h are shown in Supplementary Table 1. Unprocessed blots are shown in Supplementary Figure 8.

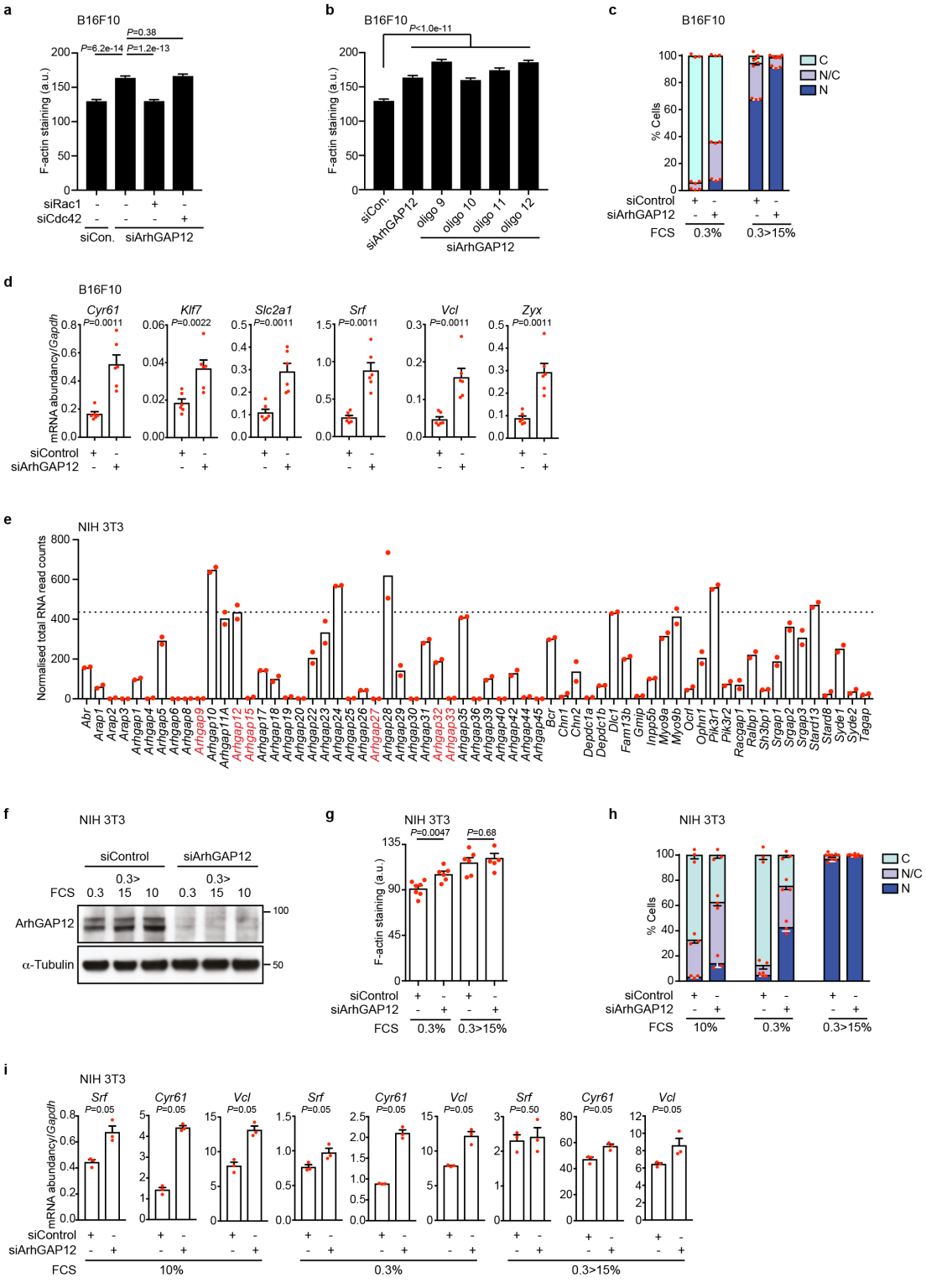

Supplementary Figure 5

ArhGAP12 controls actin dynamics in B16F10 and NIH3T3 cells.

(**a**-**d**) B16F10 cells were transfected with control or ArhGAP12 siRNA. (**a**,**b**) F-actin level in cells plated overnight on gelatin following (**a**) transfection with Rac or Cdc42 siRNA (>30,000 cells were imaged per condition) or (**b**) deconvolution of the pool of four ArhGAP12 RNAi oligonucleotides (>27,000 cells were imaged per condition). 4 fields per well have been imaged and averaged. Data shown represent *n*=24 independent wells pooled from three independent experiments. Data are means ± SEM, two-tailed Mann-Whitney test. The first two bars displayed in (a) and (b) are identical. (**c**) MRTF-A subcellular localisation in starved (0.3%) and serum-stimulated (15%, 30 min) cells. Data are means ± SEM. At least 600 cells per condition from *n*=3 independent experiments. (**d**) MRTF/SRF target gene transcription, relative to that of *Gapdh*, measured by quantitative RT-PCR using intronic primers in serum-stimulated cells (15%, 30 min). Data are means ± SEM, *n*=6 independent experiments, one-tailed Mann-Whitney test. (**e**) Expression of all rhoGAPs in serum-starved NIH 3T3 fibroblasts, from 2 independent data sets of published RNAseq expression data[16] (accession GSE45888). Dotted line indicates *Arhgap12* expression level. (**f**-**i**) Starved (0.3%), growing (10%) and serum-stimulated (15%, 30 min) NIH 3T3 cells were transfected with control or ArhGAP12 siRNA. (**f**) Representative immunoblot of three independent experiments showing the level of ArhGAP12 knockdown. (**g**) F-actin levels. 16 fields per well have been imaged and averaged. Data shown represent *n*=6 independent wells. At least 10,000 cells were imaged per condition. Data are means ± SEM, two-tailed Mann-Whitney test. (**h**) MRTF-A subcellular localisation. Data are means ± SEM, at least 150 cells per condition from *n*=3 independent experiments. (**i**) mRNA expression of MRTF/SRF target genes as in (d). Exonic primers were used. Data are means ± SEM, *n*=3 independent experiments, one-tailed Mann-Whitney test. Source data for a-d, g, h and i are shown in Supplementary Table 1. Unprocessed blots are shown in Supplementary Figure 8.

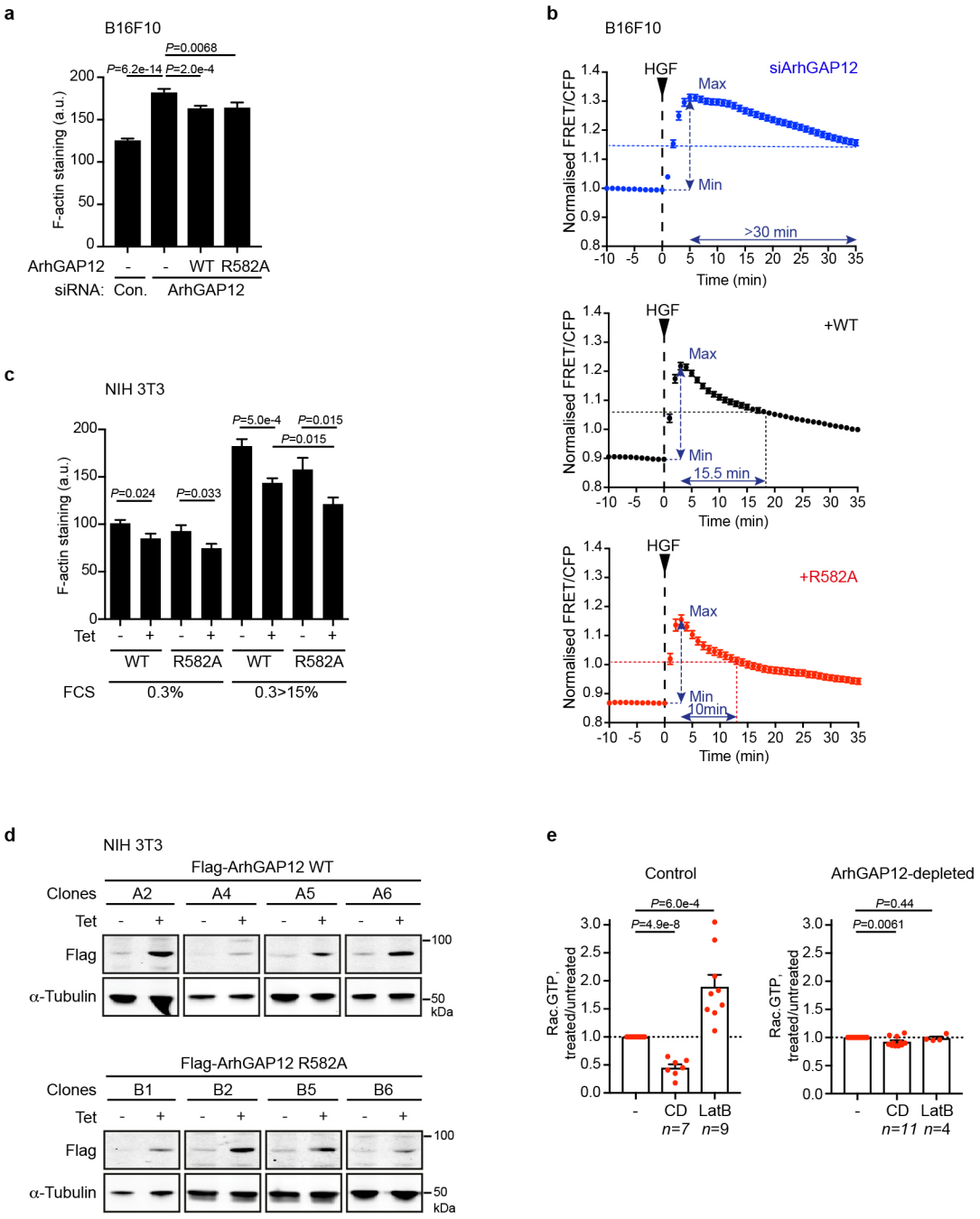

Supplementary Figure 6

G-actin regulates Rac activity through ArhGAP12.

(**a**) F-actin levels in B16F10 inducible lines stably expressing control or siRNA-resistant ArhGAP12 derivatives, transfected with control or ArhGAP12 siRNA, and plated overnight on gelatin. 4 fields per well have been imaged and averaged. Data shown represent *n*=24 independent wells pooled from three independent experiments. At least 25,567 cells were imaged per condition. Data are means ±

SEM, two-tailed Mann-Whitney test. (**b**) Kinetics of GTP loading on Rac following HGF stimulation analysed using the RaichuEV-Rac FRET biosensor for the individual conditions displayed as in Figure 7c. The time to downregulate to 50% of peak activity (t_{50}) for each curve was calculated as t_{50} = t(Min + 50% (Max - Min)) - t(Max) where t represents time, Min the minimum value, Max the maximum value. (**c**) F-actin levels in NIH3T3 Tetracycline-inducible cells stably expressing siRNA-resistant Flag-ArhGAP12 WT or R582A. 16 fields per well have been imaged and averaged. Data shown represent *n*=12 independent wells. At least 5,700 cells were imaged per condition. Data are means ± SEM, two-tailed Mann-Whitney test. (**d**) Immunoblot showing the expression of Flag-ArhGAP12 in the different NIH3T3 lines used in (c) (4 each). (**e**) Summary of the effects of ArhGAP12 knockout or siRNA-mediated depletion on CD- or LatB-induced changes in Rac GTP loading. Data from all the conditions tested in Figure 7 were pooled according to ArhGAP12 status. Data are means ± SEM, *n*, independent experiments as indicated, two-tailed unpaired t test. Source data for a-c and e are shown in Supplementary Table 1. Unprocessed blots are shown in Supplementary Figure 8.

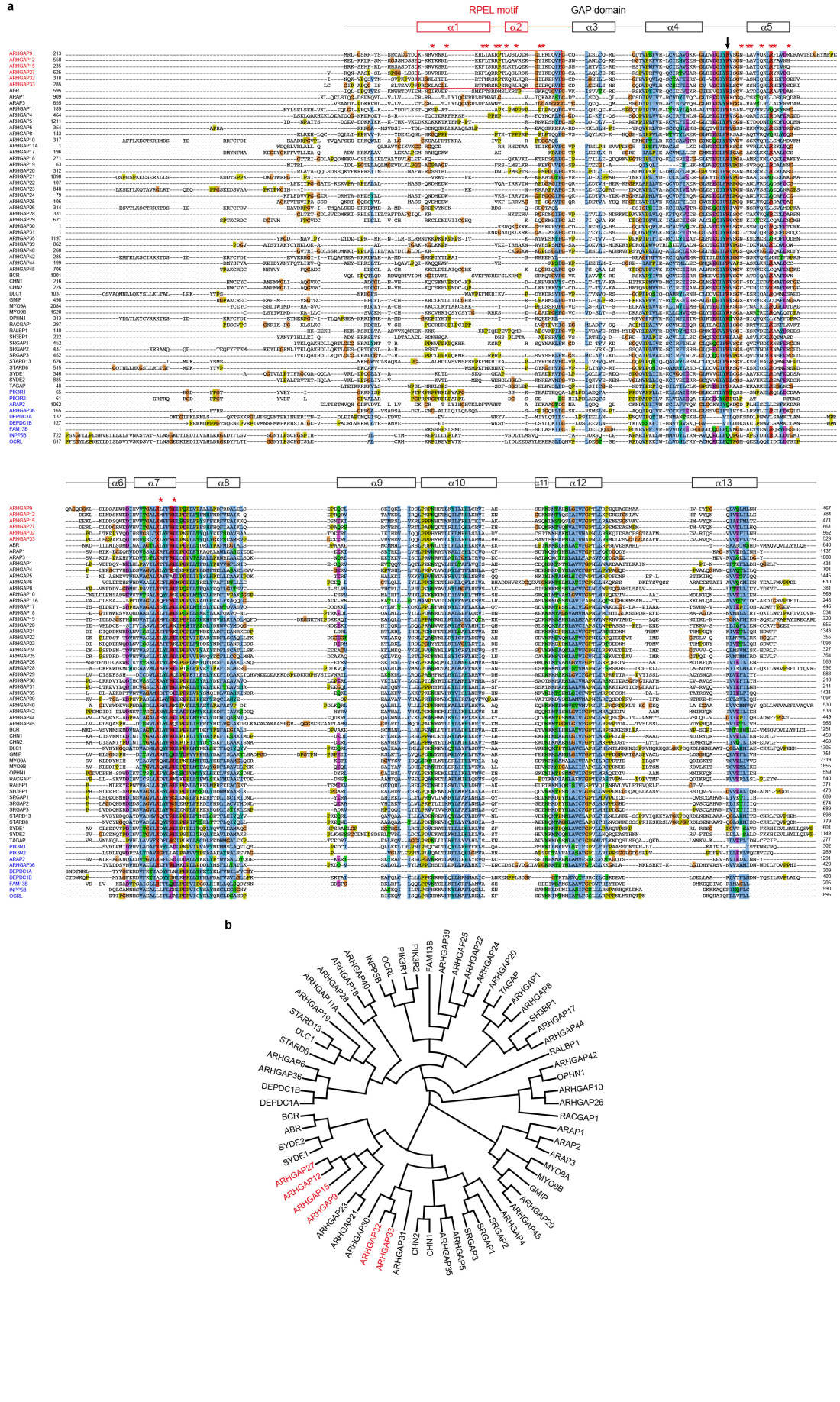
a
RPEL motif
GAP domain
α1
α2
α3
α4
α5
α6
α7
α8
α9
α10
α11
α12
α13
ARHGAP9
ARHGAP12
ARHGAP15
ARHGAP27
ARHGAP32
ARHGAP33
ABR
ARAP1
ARAP3
ARHGAP1
ARHGAP4
ARHGAP5
ARHGAP6
ARHGAP8
ARHGAP10
ARHGAP11A
ARHGAP17
ARHGAP18
ARHGAP19
ARHGAP20
ARHGAP21
ARHGAP22
ARHGAP24
ARHGAP25
ARHGAP26
ARHGAP28
ARHGAP29
ARHGAP30
ARHGAP31
ARHGAP35
ARHGAP39
ARHGAP40
ARHGAP42
ARHGAP44
BCR
CHN1
CHN2
DLC1
GMP
MYO9A
MYO9B
OPHN1
RACGAP1
RALBP1
SH3BP1
SRGAP1
SRGAP2
SRGAP3
STARD13
STARD8
SYDE1
SYDE2
TAGAP
PIK3R1
PIK3R2
ASAP2
ARHGAP36
DEPDC1A
DEPDC1B
FAM13B
INPP5B
OCRL
b
PIK3R1
PIK3R2
FAM13B
ARHGAP39
ARHGAP25
ARHGAP22
ARHGAP24
ARHGAP20
TAGAP
ARHGAP1
ARHGAP8
SH3BP1
ARHGAP17
ARHGAP44
RALBP1
ARHGAP42
OPHN1
ARHGAP10
ARHGAP26
RACGAP1
ARAP1
ARAP2
ARAP3
MYO9A
MYO9B
GMP
ARHGAP29
ARHGAP5
ARHGAP4
SRGAP2
SRGAP3
ARHGAP35
CHN1
CHN2
ARHGAP31
ARHGAP33
ARHGAP32
ARHGAP30
ARHGAP21
ARHGAP23
ARHGAP9
ARHGAP15
ARHGAP12
ARHGAP27
SYDE1
SYDE2
ABR
BCR
DEPDC1A
DEPDC1B
ARHGAP36
ARHGAP6
STARD8
DLC1
STARD13
ARHGAP11A
ARHGAP28
ARHGAP18
ARHGAP40
INPP5B
OCRL

Supplementary Figure 7

Mouse rhoGAP proteins.

(a) Multiple sequence alignment. The alignment of mouse rhoGAP domains, with the 50 residues preceding them was generated using default parameters in Clustal Omega and implemented in Jalview with the Clustal X colour scheme. RPEL-containing proteins are indicated in red; rhoGAP-like proteins lacking GAP activity, or the arginine finger or key residues for the binding of rho GTPases are indicated in blue as described previously[10]. Black arrow, catalytic arginine finger. Red asterisks highlight residues of ArhGAP12 which make contact with actin. The secondary elements of ArhGAP12 are presented on the top of the alignment. **(b)** Phylogenetic tree. A Clustal Omega-multiple sequence alignment of each GAP domain including its preceding 50 residues, was used to generate the phylogenetic tree by the neighbour-joining clustering method. RPEL-containing proteins are indicated in red. The circular cladogram was drawn using Dendroscope.

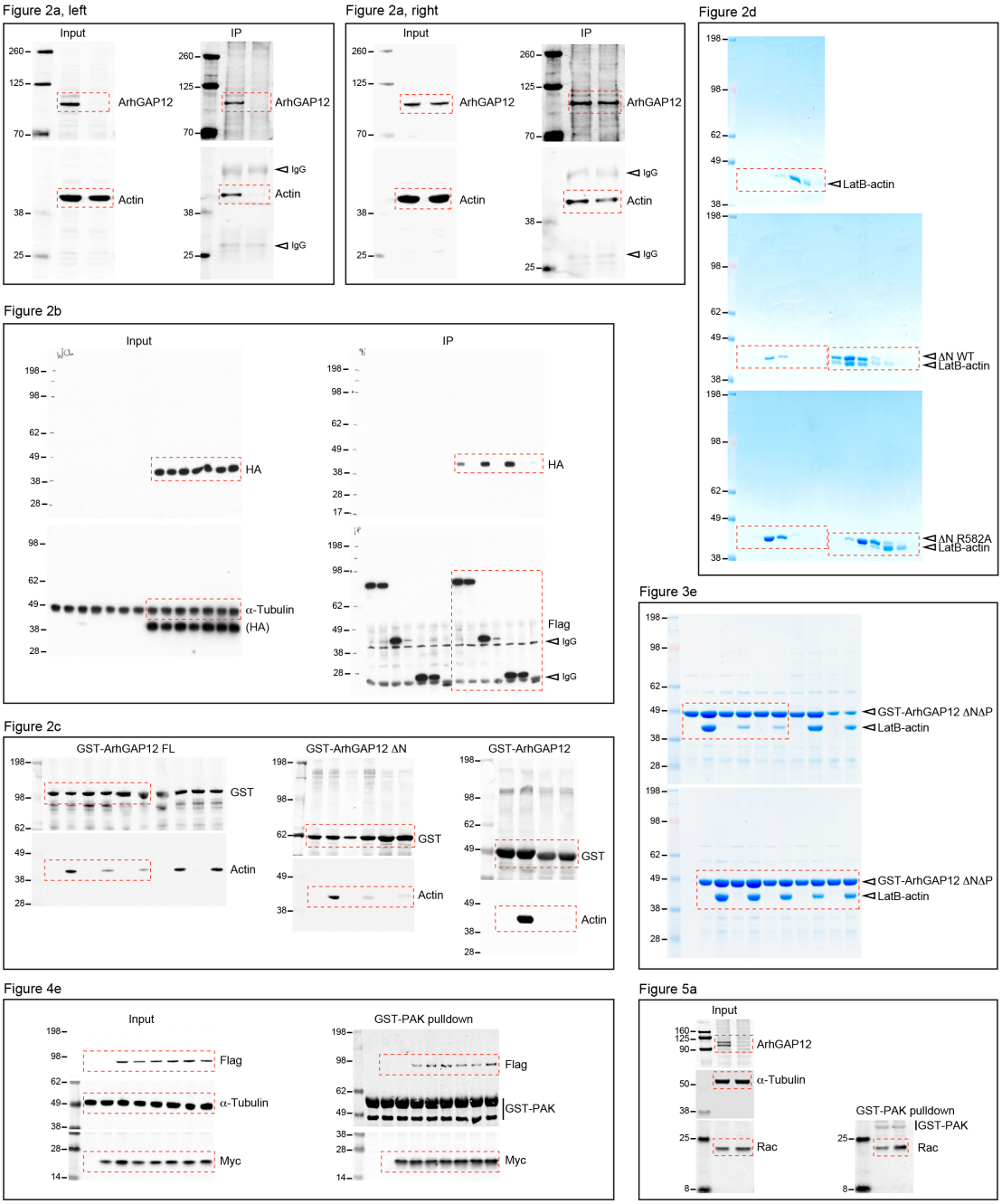

Supplementary Figure 8

Unprocessed scans of immunoblots and Coomassie gels.

Red boxes show cropped regions. Molecular weights (kDa) are indicated.

Supplementary Figure 8

Unprocessed scans of immunoblots and Coomassie gels, continued.

Red boxes show cropped regions. Molecular weights (kDa) are indicated.

Supplementary Table 1

Statistics source data.